Computational Design of a Peptide Inhibitor for Amyloid Beta (Aβ) Aggregation in Alzheimer's Disease

By

Gözde Eskici

A Thesis Submitted to the

Graduate School of Engineering

In Partial Fulfillment of the Requirements for

The Degree of

Master of Science

In

Computational Sciences and Engineering

Koç University

September 2010

Koç University

Graduate School of Sciences and Engineering

This is to certify that I have examined this copy of a Master's thesis by

Gözde Eskici

and have found that it is complete and satisfactory in all respects,

and that any and all revisions required by the final

examining committee have been made.

Committee Members:

_____

Burak Erman, Ph. D. (Advisor)

_____

Özlem Keskin, Ph. D.

_____

Türkan Haliloğlu, Ph. D

Date: _____

ABSTRACT

The most common form of dementia, Alzheimer's disease, that is neurodegenerative and incurable, is associated with tight packaging of amyloid fibrils. This packaging is caused by the compatibility of the ridges and grooves on the amyloid surface that are composed of β-sheets orientation. The major factor which creates compatibility between two amyloid surfaces is GxMxG motif. Therefore, this motif is an important target in designing inhibitors for amyloid fibrillization. In this study, particular peptides that bind Aβ40 fibrils according to amino acids groups were modified, and a small peptide library was composed. The peptide sequences that bind the surface via GxMxG motif were identified with the docking program GOLD. The sequence that had the highest docking score and binds to around MET35 was selected. Finally, the binding free energies of modified and unmodified peptides were calculated with Steered Molecular Dynamics by using the Jarzynski's Equality.

ÖZET

En yaygın demans türü olan Alzheimer Hastalığı nörodejenaratif özellik gösterir ve tedavisi mümkün değildir. β-sheet dizilimi ile oluşan amyloid proteinlerinin yüzeylerindeki girinti ve çıkıntılar birbirlerini tamamlayıcı özellik gösterir ve bu uyum Alzheimer Hastalığının ilişkili olduğu amyloid fibrillerinin sıkı bağlanmasına neden olur. İki amyloid proteinin yüzeyindeki uyumu sağlayan temel faktör GxMxG motifidir. Bu nedenle bu motif amyloid birikime karşı geliştirilecek ilaçlar için önemli bir hedeftir. Bu çalışmada, Aβ40 fibrillerine bağlanan belli peptidler amino asit gruplarına göre değiştirilmiş ve küçük bir peptid kütüphanesi elde edilmiştir. Yüzeye GxMxG motifi aracılığı ile bağlanan peptid dizileri GOLD isimli docking programı ile belirlenmiştir. Yüksek skora sahip ve MET35 civarına bağlanan peptid seçilmiştir. Seçilen peptid ile kaynak alınan peptidin bağlanma serbest enerjileri, Jarzynski eşitliği kullanılarak, Steered Moleküler Dinamik yöntemi ile hesaplanmıştır.

ACKNOWLEDGEMENTS

I am deeply thankful to my supervisor, Prof. Burak Erman, whose encouragement, guidance, and support from the beginning of this research project to the its final completion enabled me to develop a new understanding of the challenging subject. I appreciate his effort in directing me to the area of drug design; and I consider it an honor to have been a member of his research group.

I would like to express my gratitude to Dr. Mert Gür, who made available his support in a number of ways. I would also like to thank him for his precious friendship.

I am indebted to my colleagues and friends, Mehmet Ali Öztürk, Musa Özboyacı, Gözde Kaynak and Beytullah Özgür for everything that we have shared. These two years that we spent together is unforgettable.

Special thanks should also be given to my great friends Esra Aynacı, Okan Harman, Emrah Ürel, and Sedef Dinçer, who have been special supporters of this project.

I owe my deepest gratitude to my family: This thesis would not have been possible without their love and encouragement. I would like to offer my regards and blessings to Zeki Eskici, Fazilet Eskici, and Görkem Eskici, who have supported me in all respects throughout my educational life.

Finally, words cannot express the thanks I owe to Haluk Özbay, for his presence, encouragement, assistance, and love.

October 2010

TABLE OF CONTENTS

LIST OF TABLES

LIST OF FIGURES

INTRODUCTION

Alzheimer's disease (AD), first described by the neuropathologist, Alois Alzheimer, and named after him [1], is the most common type of dementia [2]. It causes failure of intellectual functions and recent memory [3], which are characteristic features of AD. When a patient has these signs, diagnosis can be confirmed by cellular pathology and cognitive tests [4]. Reductions in brain size, because of the loss of neurons and synapses, and clearly visible amyloid plaques confirm the presence of AD [5,6].

In this study, the aim was to develop peptide drugs which act against amyloid fibrillization. The reference point was a particular peptide sequence [7] that binds to amyloid fibrils experimentally. The residues of this peptide were changed with other amino acids in the same amino acid group. The amino acids groups separate amino acids according to their side chains' chemical properties. Thus, a small library was composed and the peptide sequences in this library were docked to Aβ42 protofilament subunit (pdb accession code 2BEG) by using GOLD 4.1.1 (Genetic Optimization for Ligand Docking)[8]. The one that had the highest docking score and fits in glycine grooves in GxM(35)xG motif was selected.

The docking provided specific conformation of peptide and protein with the binding score. These specific conformations of the complexes of Aβ42 protofilament subunit with modified and unmodified peptides were used as initial structures. They were solvated and equilibrated with molecular dynamics simulations by using Isothermal-Isobaric (NPT) ensemble and Canonical ensemble (NVT). By considering the Root Mean Square Deviation (**RMSD**) change of peptide, sample conformations from canonical ensemble, each being 0.25 ns separate from each other were taken as starting structures for SMD simulations. The peptides in the complexes were pulled with constant velocity by using Steered Molecular Dynamics. Finally, the average binding free energies of peptides were calculated with Jarzynski's Equality.

Chapter 1 provides more detailed background information on β- amyloid aggregation and the GxMxG motif. The methodology and the computational tools of this methodology are summarized.

Chapter 2 describes the methodology and the approaches that are used in computational tools and calculations in details. A brief theoretical background is given for molecular docking and molecular dynamics simulations.

Chapter 3 introduces the results. The docking scores, analysis of RMSD, results of Steered Molecular Dynamics and calculated binding free energies are included in this chapter.

Chapter 4 discusses and explains the results.

Chapter 5 presents the conclusion of this research project for purposes of this thesis.

CHAPTER 1

OVERVIEW

1.1. ALZHEIMER'S DISEASE

Alzheimer's disease (AD), the most common type of dementia [2], is an irreversible, progressive brain disease, which has destructive effects on memory and thinking [9]. AD was first described by the Bavarian neuropathologist, Alois Alzheimer, in a 51-year-old woman [1]. Warning signs of AD are difficulties in speaking, writing, planning, understanding visual images, and performing familiar tasks. Changes in personality follow the changes in memory [10]. When a patient has these characteristic signs, diagnosis can be confirmed by cellular pathology and cognitive tests [11,12]. Because AD cannot be identified by a single test, a medical history and physical examination are also necessary for diagnosis [10]. Reductions in brain size because of the loss of neurons and synapses (Figure 1.1.1) [13] and clearly visible amyloid plaques (Figure 1.1.2) [14] confirm the presence of AD [5,6].

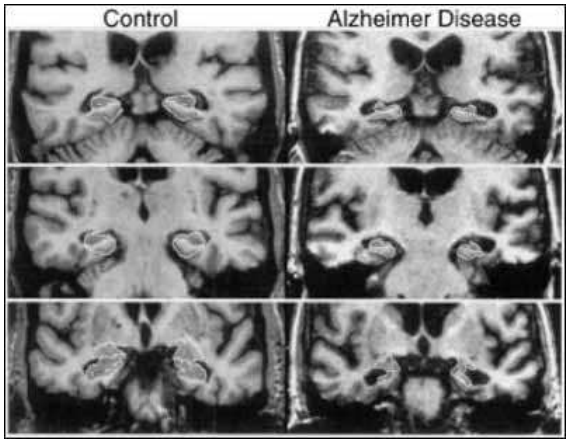

FIGURE 1.1. 1* : *Comparison of brain sizes. (Left – normal brain, right- brain with AD)[13]

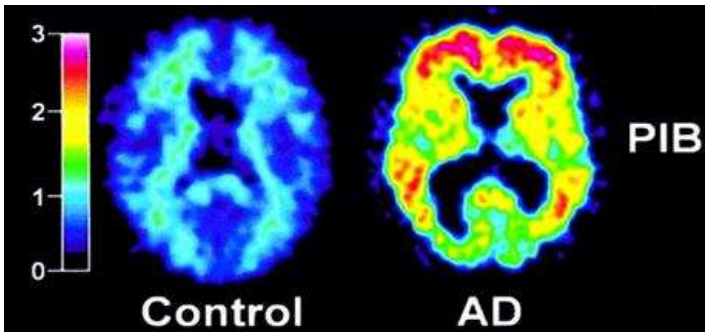

FIGURE 1.1. 2 : Imaging brain amyloid in Alzheimer's disease with Pittsburgh Compound-B [14]

For many AD cases, the causative factor is not clear. It develops as a result of multiple causes and the greatest risk factor is age. Rarely is AD familial: the causative reason is the inheritance of mutant chromosome 21. This type of Alzheimer's occurs early in life. The most common type of AD that occurs late in life does not have one specific reason. However, research shows that amyloid plaques in the brain are the major players in the pathophysiology. The first proof for this hypothesis comes from the fact that people with Down Syndrome who have an extra copy of the amyloid beta precursor protein (APP), almost without exception have AD [15,16]. Furthermore, studies with transgenic mice that have the mutant form of the APP gene produce amyloid plaques and have difficulties in learning [17,18].

In 2008, there were approximately 30 million people worldwide who diagnosed with AD. Researchers assume that this number will increase to over 100 million by the year 2050 [19]. Unfortunately, AD is incurable now. Available treatments retard the progress of the disease by increasing the concentration of acetylcholine (ACh). One of the significant features of AD is the reduction of acetylcholine by the death of cholinergic neurons [20]. Donepezil (brand name *Aricept*) [21], galantimine (*Razadyne*) [22] and rivastigmine (*Exelon*) [23] are cholinesterase inhibitors that have been used as drugs for AD. In addition to showing no effect in delaying the onset of AD, these drugs have side effects that include vomiting, muscle cramps, bradycardia, and decreased appetite [24,25,26,27].

1.1.1. BETA AMYLOID

Senile plaques, which are structurally complex lesions, are not completely understood. After the amorphous phase of senile plaques, they become aggregates of a 40- to 42-residue

protein that is called the amyloid β protein (Aβ) [28]. These 40- to 42-residue proteis are an abnormal cleavage product of APP called amyloid-β peptide (Aβ). The amyloid fibril consists of 39-43 amino acids. α-, β- and γ-secretases which can cut APP in to different parts. As seen in Figure 1.1.3, the amyloidogenic process is performed by sequential cleavage by β- and γ-secretases [29].

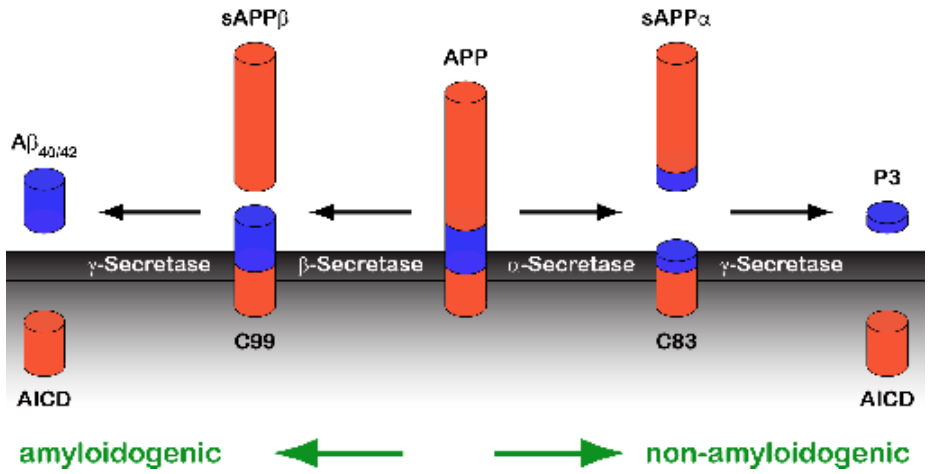

FIGURE 1.1. 3 : Enzymatic processing of APP. (Aβ40/42 is amyloid β peptide with 40 or 42 amino acid residues; AICD is APP intracellular domain; APP is amyloid precursor protein; sAPPα is soluble APP after α-secretase cleavage; sAPPβ is soluble APP after β-secretase cleavage.)[29]

Later, Aβ aggregates become fibrillar, and classical features of amyloid plaques become distinctive. They are composed of compact bundles of ~8-nm filament via -pleated sheet protein conformation. Many dendritic processes and dystrophic axons are placed around the fibrous amyloid deposit. The most reliable and significant indicator for the presence of AD is the large amount of senile or neurotic plaques in limbic and association cortices [28].

Aβ has been studied by using many different experimental and theoretical methods [29].The computational and experimental models of structures with a U-turn bent β-sheet were appeared in the 1990s [30, 31]. Models revealed that the side chain of I32 lies toward the b-turn whereas the side chain of M35 lies outward. Models further show that the side chain of M35 has an important role in gaining neurotoxic properties of Aβ [32, 33]. Figure 2.1.4 shows that the tightly formed steric zipper via two M35 residues in two different antiparallel amyloid proteins leads to sheet-to-sheet packaging. Therefore this association is a logical target in developing inhibitors to prevent aggregation [7].

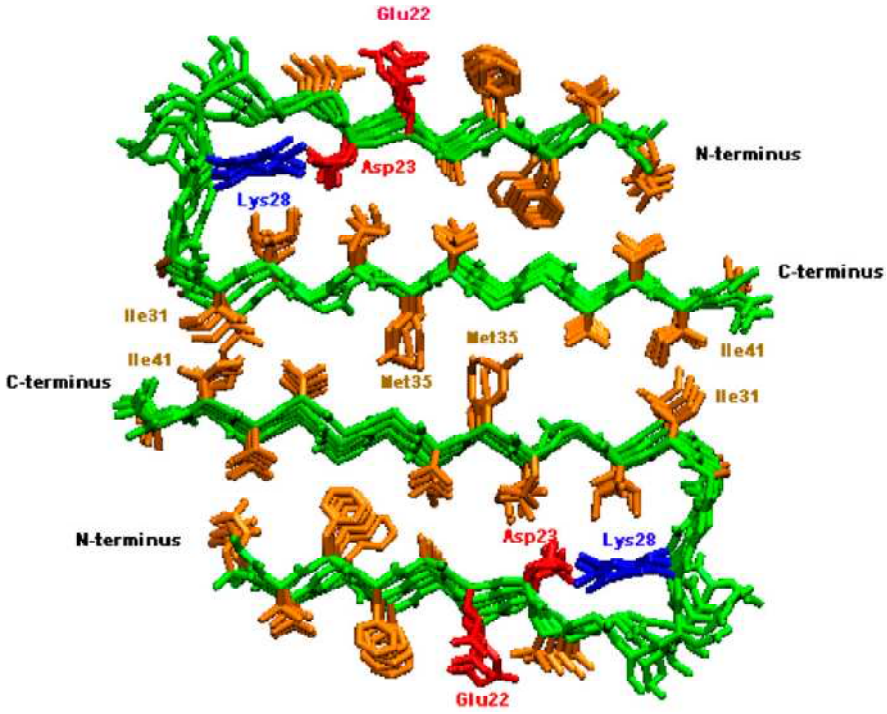

FIGURE 1.1. 4 : Sheet- to- sheet packaging of two antiparallel β-amyloid via M35 – M35 association[33]

1.2. PEPTIDE DRUGS

Peptides are short amino acid sequences that play an active role in regulation. Hence, they are promising for future drug research. Recent developments and manufacturing improvements have made peptides more stable. According to investigations, more than 40 peptides are marketed, almost 270 peptides are tested clinically, and almost 400 peptides are in advanced preclinical phases. Commonly used proteins, such as, oxytocin, insulin, cyclosporine, and vancomycin are all peptide-based drugs [35].

Peptide drugs have higher a activity and higher specificity than chemical drugs. Moreover, toxicity, which is an important factor for drug development, is lower for peptide-based drugs. On the other hand, peptide drugs also have some disadvantages, such as, less stability, low solubility, and high digestibility. The advantages and disadvantages of peptide drugs are listed in Table 1 [35].

TABLE 1: The advantages and disadvantages of peptide drugs [35]

PEPTIDE PROS AND CONS	
Advantages	Disadvantages
High activity	Low oral bioavailability
High Specificity	Injection required
Little unspecific binding to molecular structures other than desired target	Less stable
Minimization of drug-drug interactions	Diffucult delivery : challenge to transport Across membranes
Less accumulation in tissues	Challenging & costly synthesis
Lower toxicity	Solubility challenges
Often very potent	Risk of immunogenic effects
Biological & chemical diversity	Cleared from body quickly

1.3. COMPUTATIONAL BACKGROUND

1.3.1. MOLECULAR DOCKING

In early-phase drug discovery studies, novel drugs are identified by screening large molecule libraries. Since there are some experimental problems that affect the complexity of the assay procedure, the cost, and screening quality [36,37,38,39], the computational screening methods become important tools with recent improvements in computational techniques and the advancement of computer performance, structure based screening has become a commonly used method in drug development.

The principal of structure based computational methodology is based on molecular docking. The premise behind molecular docking is the prediction of the conformation of a protein-ligand complex and the presentation of binding affinity as a docking score. The docking programs; therefore, generally have two operations: docking and scoring. In the first operation, multiple protein-ligand conformations or multiple ligand conformations in defined binding pocket in receptor protein are produced [40-46]

Most of docking programs keep the receptor protein in fixed conformation and allow ligand to rotate [47]. Secondly, the binding affinity between the receptor protein and the ligand is calculated with a scoring function [48, 49]. Although, the docking programs are fast and essential tools, the results can include false positives [50].

The discussions about the problems of molecular docking include the inaccuracy of scoring functions, flexibility, and neglecting the solvent-related terms. Moreover, the docking score based on the binding free energy is not an accurate result, as it is calculated for a single conformation instead of evaluating it as an ensemble property [51].

1.3.2 MOLECULAR DYNAMICS

For 25 years, molecular dynamic simulations have been essential tools for the analysis of the structure and function of biological macromolecules. Molecular dynamics simulations provide coordinates of an individual particle as a function of time. This makes molecular dynamics simulations very important for biophysics. Another significant feature is that the system is under the control of the user. Thus, the user can remove or change specific contributions of potentials [52].

To confirm results of molecular dynamics simulations, the ergodic hypothesis of statistical mechanics is used. According to this hypothesis, averages of statistical ensemble are the same as the time averages of the system, so it is mainly based on statistical mechanics [53].

The essential task of molecular dynamics simulations is to solve the classical equations of motion numerically. For a simple atomic system these classical equations may be written :

$$m_i \ddot{r}_i = f_i \qquad \text{Eq 1. 1}$$

$$f_i = -\frac{\partial}{\partial r_i} U \qquad \text{Eq 1. 2}$$

Calculation of the forces f_i acting on the atoms can be derived from a potential energy U (r^N). The complete set of 3N atomic coordinates is represented with $r^N = (r_1,r_2,r_3 \ldots r_N)$ [54]. Recently, in the studies of biomolecular systems, molecular dynamics simulations are commonly used to get detailed information about atomic interactions and fluctuations [55]. With the improvements that have made force fields more reliable, the results of molecular dynamics simulations are more realistic. MD simulations are mainly used in identifying the dynamics, time averaged properties, and thermodynamically possible conformations [52].

CHAPTER 2

COMPUTATIONAL METHODS

2.1. MODELS OF PROTEIN AND PEPTIDE

In amyloid literature, the terms “fibril” and “protofilament” refer to different degrees of molecular organization of biological fibers. “Fibril” is generally used for the lowest degree of organization. In studies of Amyloid proteins, it refers to organization between many of protein chains that have different sizes and are still soluble. They have unknown degree of complexity [56]. On the other hand, the term “protofilament” refers to assembled fibrils that are perpendicular to the fibril axis in two molecular layers. [7,57,58]. Here, we study the inhibition of association of two Aβ protofilament to form the mature fibril and the terms “fibril” and “protofilament” are used interchangeably.

2.1.1 AMYLOID BETA – 42

In this study, Aβ42 protofilament subunit (pdb accession code: 2BEG) was used for docking and molecular dynamics simulations. The 3D structure of the fibrils comprising Aβ (1-42) was obtained by using hydrogen-bonding constraints from quenched hydrogen-deuterium exchange NMR, side-chain packing constraints from pair wise mutagenesis studies, and parallel, in-register -sheet arrangement from previous solid state NMR studies [58]. In this used pdb file (2BEG), there are ten chains. One of them (model 1) was used for docking and molecular dynamics simulations (Figure 2.1)

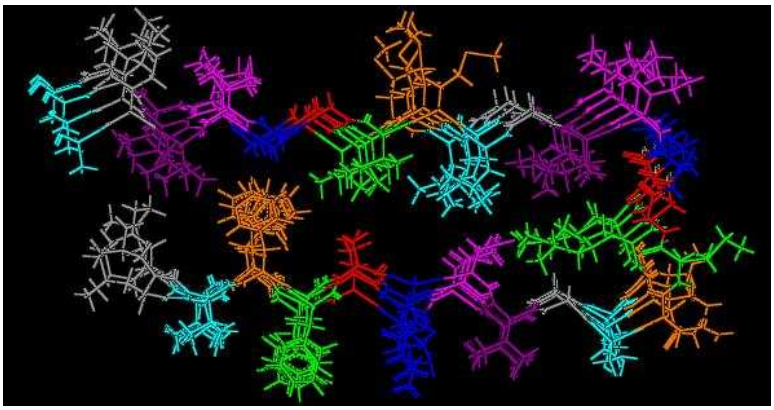

FIGURE 2. 1 : Model A in PDB file (2BEG)

2.1.2 THE REFERENCE PEPTIDE (INH1)

Amyloid fibrils have a defining characteristic spatial organization, called cross β-sheet that is formed by the association of β-strands [59]. The term cross-β fibril, refers to the overall structure where individual β strands have in-register and parallel arrangement [60]. Three consecutive repeats of GxxxG motif may take place in peptide accumulation [61] and form molecular ridges and grooves in the surface. These are critical for rational design of inhibitors to prevent fibril formation [7].

The GxxxG motif is also found in prion protein [62] and α-synuclein protein [63]. In order to understand the role of glycine and the importance of the GxxxG motif, a model peptide (GpA70-86) that is composed of spanning residues of transmembrane helix of glycophorin A, was studied experimentally. This model peptide has also in-register orientation like other amyloids, and it contains GxxxG motif between residues 79 and 83. The study showed that the amino acids with large side chains form molecular ridges which fit into the glycine grooves. The compatibility between surfaces stabilizes fibril formation. [7]

Smith et al studied a model peptide that has the general inhibitor architecture RGTFEGKF-NH_2 and showed that this inhibitor prevents GPA70-86 and Aβ fibrillization. [7] The inhibitor is designed in a way that the hydrophobic xGxFxGxF and hydrophilic RxTxExKx amino acids are placed on the opposite faces of the peptide. Thus, the small and large amino acids on the hydrophobic face of the inhibitor match the GxxxG face of the Aβ peptide. Moreover, variants of this peptide also affect Aβ fibrillization negatively. [7]

2.2. PEPTIDE LIBRARY

In this research, the architecture of the experimentally successful reference peptide [7] was modified by changing its amino acids, with other amino acids which are in the same group according to their side chains. These groups are formed according to chemical properties of radical groups of amino acids. The reference grouping system is given in Table 2.

TABLE 2: The grouping system that was used in this study*

		pK_a values				
Amino Acid	**Symbol**	**pK_1**	**pK_2**	**pK_R**	**Hydropathy index**	**Occurrence in Proteins (%)**
Nonpolar, aliphatic R groups : The amino acids in this group have non-polar hydrophobic side chains. They use hydrophobic interactionsto stabilize protein structure						
Glycine	Gly G	2.34	9.60		-0.4	7.2
Alanine	Ala A	2.34	9.69		1.8	7.8
Proline	Pro P	1.99	10.96		1.6	5.2
Valine	Val V	2.32	9.62		4.2	6.6
Leucine	Leu L	2.36	9.60		3.8	9.1
Isoleucine	Ile I	2.36	9.68		4.5	5.3
Methionine	Met M	2.28	9.21		1.9	2.3
Aromatic R groups : Amino acids of this group have a cyclic structure intheir side chains, and these side chains are relatively hydrophobic						
Phenylalanine	Phe F	1.83	9.13		2.8	3.9
Tyrosine	Tyr Y	2.20	9.11	10.07	-1.3	3.2
Trptophan	Trp W	2.38	9.39		-0.9	1.4
Polar, Uncharged R groups : The side chains of these amino acids are more soluble in water, therefore they form hydrogen bonds with water						
Serine	Ser S	2.21	9.15		-0.8	6.8
Threonine	Thr T	2.11	9.62		-0.7	5.9
Cysteine	Cys C	1.96	10.28	8.18	2.5	1.9
Asparagine	Asn N	2.02	8.80		-3.5	4.3
Glutamine	Gln Q	2.17	9.13		-3.5	4.2
Positively charged R groups: These are the most hydrophilic amino acids which have significant positive charge at their side chains						
Lysine	Lys K	2.18	8.95	10.53	-3.9	5.9
Histidine	His H	1.82	9.17	6.00	-3.2	2.3
Arginine	Arg R	2.17	9.04	12.48	-4.5	5.1
Negatively charged R groups : These have a second carboxyl group with a net negative						

* Nelson, D. L & Cox, M.M. (2005). Lehninger: The principles of biochemistry. (4th Edition). New York: W.H Freeman and Company

charge at pH 7.0						
Aspartate	Asp D	1.88	9.60	3.65	-3.5	5.3
Glutamate	Glu E	2.19	9.67	4.25	-3.5	6.3

For example, to test the role of 1-Arginine in inhibition, it was changed with Histidine and Lysine (HGTFEGKF, KGTFEGKF); and to test the importance of Lysine in seventh residue, it was replaced with Arginine and Histidine (RGTFEGRF, RGTFEGHF).

Phenylalanine was replaced with Tyrosine and Tryptophan. Since there are two Phenylalanine residues, the fourth and eighth positions were changed separately and then together (RGTWEGKF, RGTYEGKF, RGTFEGKW, RGTFEGKY, RGTWEGKW, RGTYEGKY-NH_2, RGTYEGKW-NH_2, and RGTWEGKY-NH_2). Glycines in the second and sixth positions were changed only with Valine, Isoleucine, and Leucine from the amino acid group that has nonpolar, aliphatic R groups. Since the methionine derivative of peptide was not effective [7], glycine was not changed with methionine. Serine, Asparagine, Glutamine was used instead of Threonine in the third position and Aspartate was replaced with Glutamate.

After analyzing the results of one type of change, the library was expanded by trying a combination of amino acid replacements that resulted in higher docking scores. For example, the replacement of glycine with valine and the replacement of phenylalanine with Tyrosine, Tryptophan was done together. Additionally, the peptide sequences that was obtained with some random replacements of amino acids from different groups are added to peptide library.

In order to obtain PDB files of peptides, the sequences were drawn and the three dimensional structures were minimized with ChemBioOffice 2009 that is distributed by CambridgeSoft.

2.3. MOLECULAR DOCKING

Docking studies of designed peptides were carried out using GOLD Genetic Optimization for Ligand Docking) 4.1 program from Cambridge Crystallographic Data Center, UK [8]. GOLD uses genetic algorithm for docking flexible ligands into the protein binding site to explore the full range of ligand conformational flexibility with partial

flexibility of the protein[8]. The binding energy of the ligands after auto editing by GOLD was predicted with GOLD score and ChemScore that are implemented in GOLD.

The total GOLD score is calculated by considering the hydrogen bonds and van der Waals interactions between protein and ligand. The four main components of the GOLD fitness function are protein-ligand hydrogen bond energy (external H-bond), protein-ligand van der Waals energy (external vdw), ligand internal van der Waals energy (internal vdw), and ligand torsional strain energy (internal torsion). Another component that refers to ligand intramolecular hydrogen bond energy (internal H-bond) may be added, optionally. By keeping parameter at their default options, output files give a single internal energy term S (int) which is the sum of the internal van der Waals and the internal torsion [64]. The larger fitness scores are better, since the fitness score is the negative of the sum of the component terms [64].

ChemScore is derived empirically from a set of 82 protein-ligand complexes and is trained by regression against experimental affinity data. The total free energy change is calculated by the formula below [65]:

$$\Delta G_{binding} = \Delta G_0 + \Delta G_{hbond} + \Delta G_{metal} + \Delta G_{lipo} + \Delta G_{rot}$$

Each component in this formula refers to the product of a term that is related to the magnitude of a particular physical contribution to free energy [65].

$$\begin{aligned} \Delta G_0 &= v_0 \\ \Delta G_{hbond} &= v_1 P_{hbond} \\ \Delta G_{metal} &= v_2 P_{metal} \\ \Delta G_{lipo} &= v_3 P_{lipo} \\ \Delta G_{rot} &= v_4 P_{rot} \end{aligned}$$

The *V* terms symbolize the regression coefficients and the *P* terms are the various types of physical contributions to binding. The final ChemScore includes a clash penalty and internal torsion terms. Covalent and constraint scores are also considered. [65, 66]

$$ChemScore = \Delta G_{binding} + P_{clash} + c_{internal} P_{internal} + \left(c_{covalent} P_{covalent} + P_{constraint}\right)$$

2.3.1 THE RECEPTOR THAT IS USED IN DOCKİNG STUDIES

In this study, Aβ42 protofilament subunit (PDB ID: 2BEG) was used as receptor. The ligand binding site was defined as a collection of residues placed within a sphere of 20 Å around the coordinates of SD-MET35, which is an element of GxMxG motif. In order to obtain diverse conformations with a high docking score, the number of the data files was taken as 100 and did not used the early termination option. All other parameters were kept at their default values.

Docking results were compared, and the one with the lowest ChemScore was selected for molecular dynamics simulations.

2.4. MOLECULAR DYNAMICS

As mentioned previously, molecular dynamics simulations solve the classical equation of motion numerically.

$$m_i \ddot{r}_i = f_i$$

$$f_i = -\frac{\partial}{\partial r_i} U$$

The forces f_i acting on the atoms can be calculated by the derivation from a potential energy U (r^N). The complete set of 3N atomic coordinates is represented with r^N = (r_1, r2, r3…r_N). U is the total potential energy, and is the sum of the bonded and non-bonded interactions [54].

2.4.1. Non-bonded interactions:

The potential energy that is provided by non-bonded interactions can be formulated as:

$$U_{non-bonded}(r^N) = \sum_i u(r_i) + \sum_i \sum_{j>i} v(r_i, r_j) + \cdots \quad \text{Eq 2. 1}$$

Where, $u(r_i)$ term stands for an externally applied potential field. For fully periodic simulations, it is usually neglected. For the second term in the Equation 3.1., the most commonly used form is The Lennard-Jones potential and it can be written as:

$$v^{LJ}(r) = 4\varepsilon\left[\left(\frac{\sigma}{r}\right)^{12} - \left(\frac{\sigma}{r}\right)^{6}\right] \quad \text{Eq 2. 2}$$

There are two parameters in this equation which are σ, the diameter, and ε, the well depth. If electrostatic charges are available, the appropriate Coulomb Potential is also calculated [54].

$$v^{Coulomb}(r) = \frac{Q_1 Q_2}{4\pi\varepsilon_0 r} \quad \text{Eq 2. 3}$$

2.4.2 Bonded interactions:

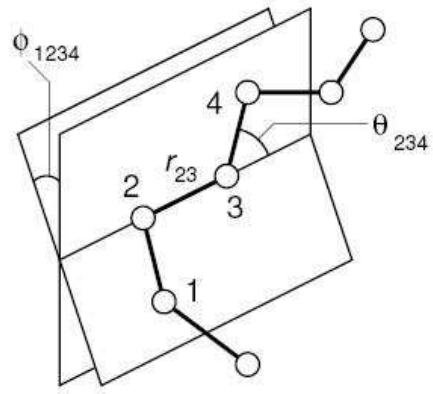

FIGURE 2.4. 1 : The Geometry of a single chain

Figure 2.4.1. shows the geometry of a simple chain molecule. The bonds between neighbor atoms is represented with $r_{ij} = |r_i - r_j|$, the bond angle between adjacent bonds, such as, $r_i - r_j$ and $r_j - r_k$ is represented with θ_{ijk}, and ϕ_{ijkl}stands for the torsional angle [54].

The potential that is caused by intramolecular forces can be formulated as:

$$U_{intramolecular} = \frac{1}{2}\sum_{bonds} k_{ij}^{r}\left(r_{ij} - r_{eq}\right)^2 + \frac{1}{2}\sum_{bond\ angles} k_{ijk}^{\theta}\left(\theta_{ijk} - \theta_{eq}\right)^2 + \frac{1}{2}\sum_{torsion\ angles}\sum_{m} k_{ijkl}^{\phi,m}\left(1 + \cos\left(m\phi_{ijkl} - \gamma_m\right)\right) \quad \text{Eq 2. 4}$$

where

$$\cos\phi_{ijk} = \hat{\boldsymbol{r}}_{ij}\cdot\hat{\boldsymbol{r}}_{jk} = \left(r_{ij}\cdot r_{ij}\right)^{-1/2}\left(r_{jk}\cdot r_{jk}\right)^{-1/2}\left(r_{ij}\cdot r_{jk}\right), \quad \left(\ \hat{\boldsymbol{r}} = \boldsymbol{r}/|r|\ \right) \quad \text{Eq 2. 5}$$

$$\cos\phi_{ijkl} = -\hat{n}_{ijk}\cdot\hat{n}_{jkl}, \quad \left(n_{ijk} = r_{ij}\times r_{jk}, \quad n_{jkl} = r_{jk}\times r_{kl}, \quad \hat{\boldsymbol{n}} = \boldsymbol{n}/n\ \right) \quad \text{Eq 2. 6}$$

The form of Equation 2.4., the strength parameters k and other constants are specified in the used force fields. The term “force field” expresses the combination of formula of molecular dynamics and associated parameters that are used in potential energy calculation [67]. There are different force fields that are commonly used in biomolecular simulations. These include AMBER [68], CHARMM [69], OPLS [70] and Dang95 [71] with SPC/E [72] and TIP3P [73] water models.

In this study, molecular dynamics simulations were performed in explicit solvent (water) using NAMD 2.6 [74] with CHARMM27 [75] force field. Simulations were performed at 310 K temperature and 1 bar pressure. The highest scoring docked structures obtained in GOLD of AB1 (modified version of reference peptide) and INH1 (reference peptide) were selected as their initial structures.ACE cap were used for the N-terminus and CT3 cap were used for the C-terminus . The reaction coordinates were aligned with the positive x axis. The proteins were then solvated in a waterbox of 40 **Å** cushion in the positive x direction and 10 **Å** cushions in the other directions. Periodic boundary conditions were applied. Ions were added in order to represent a more typical biological environment. Langevin dynamics was used to control the systems temperature and pressure. All atoms were coupled to the heat bath. A time step of 1fs was used.

Nonbonded and electrostatic forces were evaluated each time step. In order to keep all degrees of freedom no rigid bonds were used. At every 500th time step of final conventional

molecular dynamic simulation, the instantaneous atomic coordinates **R** of all atoms, the pressures and the energies were recorded.

2.4.1. MINIMIZATION

The pdb file along with the psf file, that is generated with NAMD, contains guessed coordinates for hydrogen atoms of the structure. Therefore, energy minimization will correct hydrogen positions in a more accurate way [76]. The minimization was performed for 30000 steps (0.03ns). The configuration file is in the appendix. (Appendix A)

2.4.1.1. FIXATION

Generally, Molecular Dynamics minimization includes fixing and releasing molecules in the system. Since the protein responds much slower than the water, fixing the protein allows the water to settle in the first step. Thus, it provides less computational effort [76]. Additionally, fixing the protein prevents possible damage that is caused by the collapse of water molecules during minimization. The fixation in this study was performed for 500000 steps (0.5 ns) under constant temperature and constant pressure conditions. The configuration file is in the appendix. (Appendix B)

2.4.1.2. HARMONIC CONSTRAINTS

During minimization, constraints can be used to fix the motion of particular atoms. Thus

- exploration of a specific region of the potential energy surface can be improved
- boundary forces can be imposed to prevent solvent molecules from escaping, and
- high- frequency vibrations can be removed [77]

In this study, the degree of harmonic constraints were diminished step by step. The constant of constraint “k” was chosen as 1, 0.5, and 0.125 successively. Totally, restraint were removed throughout 2 ns.

2.4.2. ISOTHERMAL – ISOBARIC (NPT) ENSEMBLE

In the isothermal-isobaric ensemble, the constant parameters are the number of moles (N), pressure (P), and temperature (T). In order to keep the system at constant temperature and constant pressure, a thermostat and a barostat are required. In this study, the simulations were performed according to Langevin Dynamics.

Langevin dynamics is an approach to control the system temperature/or pressure by controlling the kinetic energy of the system. The method is based on Langevin equation for a single particle:

$$m_i \frac{d^2 x_i(t)}{dt^2} = F_i\{x_i(t)\} - \gamma_i \frac{dx_i(t)}{dt} m_i + R_i(t) \qquad \text{Eq 2. 7}$$

On the right hand side, two additional terms refer to the ordinary force that the particle experiences. The particle with frictional coefficient $\gamma_i m_i$ faces a frictional damping, and this damping is represented with the second term's equation. The third term stands for random forces which may be applied to the particle. In order to keep the system's temperature, the kinetic energy is fixed with these terms [76].

Additionally, to keep the system's pressure at a constant value Langevin piston method was used. With the extended system formalism [78], the deterministic equations of motion for the piston degree of freedom are replaced with the Langevin equation. This replacement is suitable to eliminate the non-physical ringing of the volume associated with the piston mass [79].

After performing simulations with NPT ensemble, we checked the convergence of the volume and the Root Mean Square Deviation (RMSD) convergence of the protein was checked. When two graphics started to fluctuate around a small interval, we continued with Canonical ensemble (NVT). The configuration file of simulations is in the appendix (Appendix C).

2.4.3. CANONICAL ENSEMBLE

In the canonical ensemble, the number of moles (N), the volume (V) and the temperature (T) are kept at constant values. The energy of endothermic and exothermic processes is exchanged with a thermostat. In order to arrange the energy change in the system, there are different types of thermostat methods. Simulations were performed with Langevin thermostat model that is mentioned previously. The configuration file is in appendix (Appendix D).

Conventional MD simulations were performed for 18ns for AB1 (the designed peptide which is the lowest ChemScore) and for 19ns for INH1 (the experimentally successful reference peptide) so that stable conformations of the complexes were found. Using the final structures of the T,P,N simulations additional simulation under T,V,N condition were performed. For AB1 after 5.5 ns, it was observed that the complex rotated too much in the waterbox so that there was not enough water in the pulling direction. Therefore, the final structure were realigned with the x axis and resolvated under the same conditions indicated before. Minimization and equilibration were performed under T,P,N conditions keeping the protein fixed in order to relax the water in the first place. Then T,V,N simulation were performed for an additional 9 ns. For INH1 such a strong rotation were not observed and T,V,N simulation were performed for 12 ns. Starting structures for the SMD simulations were sampled from the final 2.5 ns part of the conventional MD simulations.

2.5. STEERED MOLECULAR DYNAMICS

There are many modeling methods that are applied in searching for ligand-receptor interactions [80]. The premise behind the computer simulations that provide insights to binding affinities is the idea of reversibility. Umbrella sampling and free energy perturbation are based on reversibility [81,82,83]. In Steered Molecular Dynamics, time-dependent external forces are applied, and the changes in the system are analyzed. During these processes, irreversibility is considered. Thus, it can be applied for searching ligand binding or conformational changes and give more realistic results.

Analysis of the unbinding of the ligand and the recording of applied forces can give information about ligand-receptor interaction and binding pathway. Additionally, quantitative information about the binding potential can be also obtained with SMD.

In order to apply external forces, there are different options. One of them is to restrain the ligand to a point in space. Unbinding is performed by shifting the restraint point in a specifically defined direction. Thus, the ligand is forced to move along its unbinding path. When a single reaction coordinate x, and an external potential $U = k(x - x_0)^2/2$ are assumed, the applied external force can be formulated as:

$$F = k(x_0 + vt - x) \qquad \text{Eq 2. 8}$$

In this formula, k stands for the stiffness of the restraint and x_0 expresses the initial position of the restraint point that is moving with a constant velocity v [84]. From the classical equation of work:

$$W = F \times v \times \Delta t \qquad \text{Eq 2. 9}$$

In this study, the constant velocity $\left(\mathbf{10^{-5}}\ \boldsymbol{\mathring{A}/ps}\right)$ was used and spring constant was taken as *7 kcal/mol$\mathring{A}^2$* . For designed peptides the atoms of the fifth and the sixth residues were chosen as SMD atoms, since they were the closest residues to Methionine residues on the surface of amyloid. The side chain of Methionine residue (71MET) was fixed. The simulations were performed for 3 and more nanoseconds. The configuration file is in the Appendix. (Appendix E)

2.6. POTENTIAL OF MEAN FORCE (PMF) WITH STEERED MOLECULAR DYNAMICS

In this work the unbinding of the ligand from the protein is performed with a finite velocity. Due to this finite velocity the process becomes a non-equilibrium process. The Jarzynski's Equality is a relation between equilibrium free energy differences ΔA and work done through non-equilibrium processes W[85]. The Jarzynski's Equality states that the following equality holds regardless of the speed of the process [86,87].

$$e^{-\beta \Delta A} = \langle e^{-\beta W} \rangle \quad \text{Eq 2. 10}$$

The major difficulty of the Jarzynski's Equality is that its average is dominated by small work values that are observed only rarely. Therefore, if only a small number of steered molecular dynamic simulations are performed, the velocity should be small enough to permit such small work values. In the literature, this difficulty was overcome to some extent by applying the cumulant expansion [87,88,89] as.

$$\log\langle e^{-\beta W} \rangle = -\beta \langle W \rangle + \frac{\beta^2}{2}(\langle W^2 \rangle - \langle W \rangle^2) - \frac{\beta^3}{3!}(\langle W^3 \rangle - 3\langle W \rangle^2 \langle W \rangle + 2\langle W \rangle^3) + .. \quad \text{Eq 2. 11}$$

Using the cumulant expansion, two kinds of error are involved: systematic error due to the truncation of higher order terms and statistical error due to insufficient sampling [85]. For a finite number of trajectories, the statistical error is larger than the systematic error. Therefore, as [85] have been pointed out, approximate formulas may give better results because lower order cumulants are estimated with smaller statistical error.

The finite-sampling estimate of a non-linear average is biased [85]. Therefore, instead of using the second order cumulant expansion directly, the unbiased estimate introduced by [85] will be used as:

$$\log\langle e^{-\beta W} \rangle = \frac{1}{\beta}\left\{\frac{1}{M}\sum_{i=1}^{M} W_i - \frac{\beta}{2}\frac{M}{M-1}\left[\frac{1}{M}\sum_{i=1}^{M} W_i^2 - \left(\frac{1}{M}\sum_{i=1}^{M} W_i\right)^2\right]\right\} \quad \text{Eq 2. 12}$$

Here, M is the total number of trajectories and W_i is the work obtained from the i^{th} trajectory. The average $\langle . \rangle$ is taken over the ensemble of SMD trajectories, whose initial states are sampled from the canonical ensemble, each being 0.25 ns separate from each other. i.e., structures of the N,V,T simulation, each again 0.25 ns away from each other will be used as starting structures for SMD simulations.

Constant velocity SMD simulations were performed in which the center of mass of the backbone atoms of residues 4-5 of the peptides is attached to a dummy atoms via a virtual spring with a spring constant of k. The dummy atom is then pulled with a constant velocity

into the reaction coordinate ξ, which is defined as the vector between the center of mass of the backbone atoms of the 71th residue of the protein (which were fixed) and the center of mass of the pulled atoms. Hence, the distance along the RC λ is changed with a constant velocity as: [90],

$$\lambda(t) = \lambda(0) + vt \qquad \text{Eq 2. 13}$$

Here t is time and $\lambda(t)$ is the λ parameter value at time t of the simulation. The Jarzynski's Equality provides the methodology to evaluate the free energy differences $A(\lambda(t)) - A(\lambda(0))$ using the work values $W_{\lambda(0)\to\lambda(t)}$. Hence, to calculate the potential of mean force (PMF) $\phi(\xi)$ at ξ, $W_{\lambda(0)\to\lambda(t)}$, values at different time t but being at the same reaction coordinate ξ, have to be combined. When the spring constant k of the guiding potential is sufficiently large so that the reaction coordinate follows the constraint center λ closely, the following stiff-spring approximation emerges [85]:

$$A(\lambda) \approx \phi(\lambda) \qquad \text{Eq 2. 14}$$

Hence, the PMF $\phi(\lambda)$ will be evaluated by the Jarzynski's equality using the work values $W_{\lambda(0)\to\lambda(t)}$.The external work is evaluated as:

$$W_{\lambda(0)\to\lambda(t)} = -KV \int_{\lambda(0)}^{\lambda(t)} [\xi - (\lambda(0) + vt)]dt \qquad \text{Eq 2. 15}$$

Due to the external potential applied to the SMD atoms, the conformation of the peptide will be lightly biased. Therefore, the final states will not be in equilibrium. However, to relax these final states, no external work is required. Therefore, Jarzynski's Equality can be stated in terms of transformations between equilibrium states [90].

CHAPTER 3

RESULTS

3.1. DOCKING RESULTS

The docking scores of RGTFEGKF and peptides that have higher docking score than RGTFEGKF are presented in Table 3.

TABLE 3 : Docking Scores of RGTFEGKF and its derivatives

NO	Sequence	ChemScore (kJ/mol)	Gold Score
1.	**RGTFEGKF (inh1)**	**-7.13**	**49.12**
2.	RVTWEGKF	-15.01	67.56
3.	RGTFQGKF	-14.18	65.43
4.	RGTFEGRF	-13.25	65.36
5.	RGTFWGKF	-12.04	64.59
6.	RITFEIKF	-10.86	63.48
7.	RGTWEIKW	-10.39	52.02
8.	RGSWEGKF	-10.11	52.86
9.	RGSFEGKW	-10.04	52.45
10.	RGLWEGKF	-9.74	58.43
11.	RGVFEGKW	-9.64	55.67
12.	RGTWEVKF	-9.35	59.31
13.	RGTFHGKF	-9.22	53.89
14.	RGSFEGKF	-8.95	53.07
15.	RVTWEVKF	-8.83	52.27
16.	RGTWEGKF	-8.83	49.87
17.	RGTFRGKF	-8.57	48.79
18.	RGSWEGKW	-8.20	49.26
19.	RGTFQGKW	-8.17	49.63
20.	RGTFYGKF	-7.91	48.98
21.	RGLWEGKW	-7.78	48.34
22.	RGTWNGKF	-7.76	48.82

As ChemScores of peptides are low, the best binding peptide (named AB1 and the second peptide in Table 1) was docked with AutoDock Vina 1.0 and binding affinity was calculated as -8.7 kcal/mol [91]

The second peptide in Table 2 was chosen for molecular dynamic simulations and free energy calculation by considering the score, binding region, and molecular properties. As a result of docking with GOLD, the complex of second peptide and amyloid protofilament subunit is given in Figure 3.1.1.

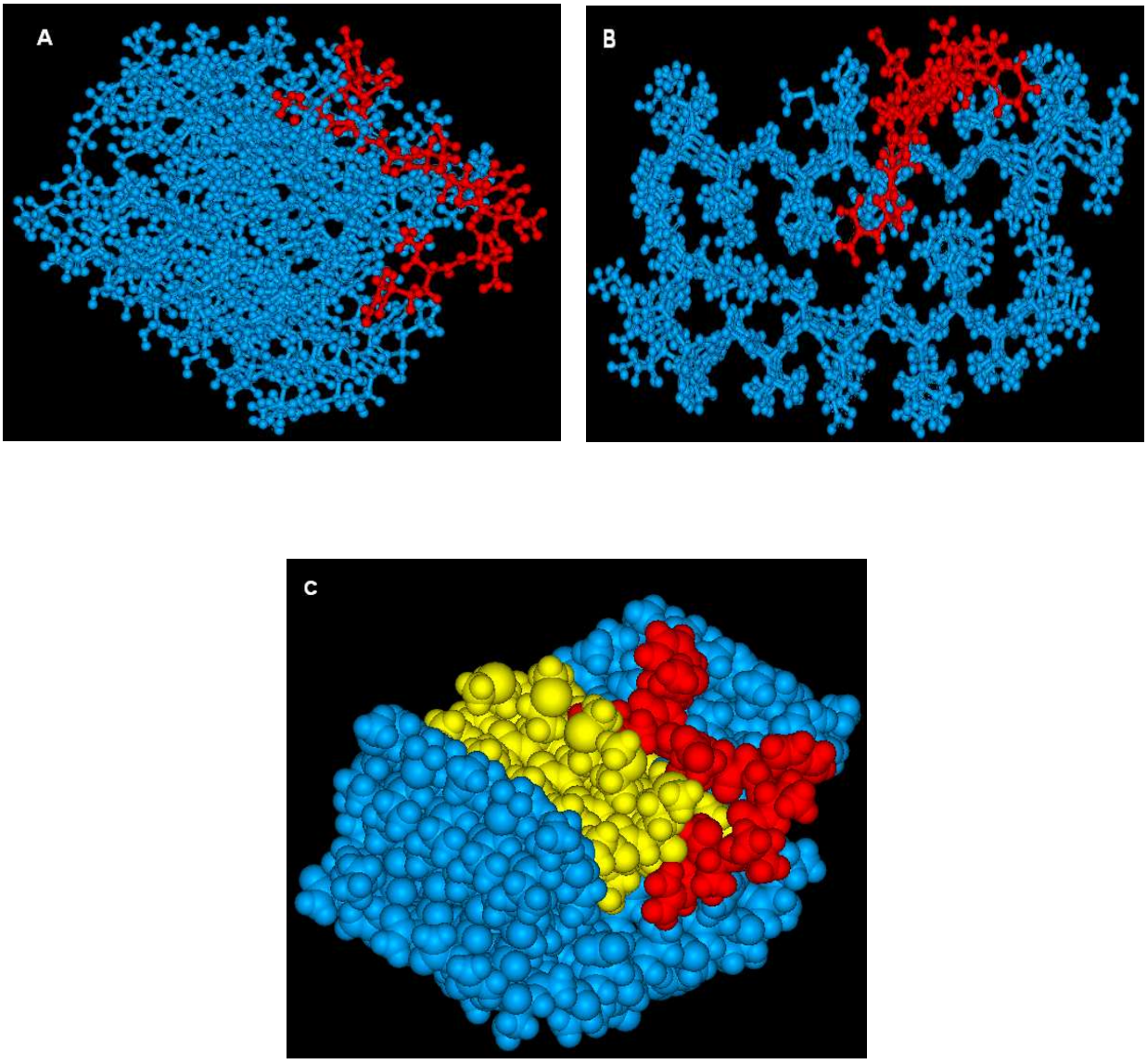

FIGURE 3.1. 1: (A-B) The complex of designed peptide (red molecule) and amyloid (blue molecule) from different sides. (C) The CPK Model of the complex. Peptide is in red and amyloid is in blue. The yellow region shows the GxMxG motif in the surface

The complex of reference peptide RGTFEGKF and amyloid protofilament subunit is shown in the Figure 3.1.2

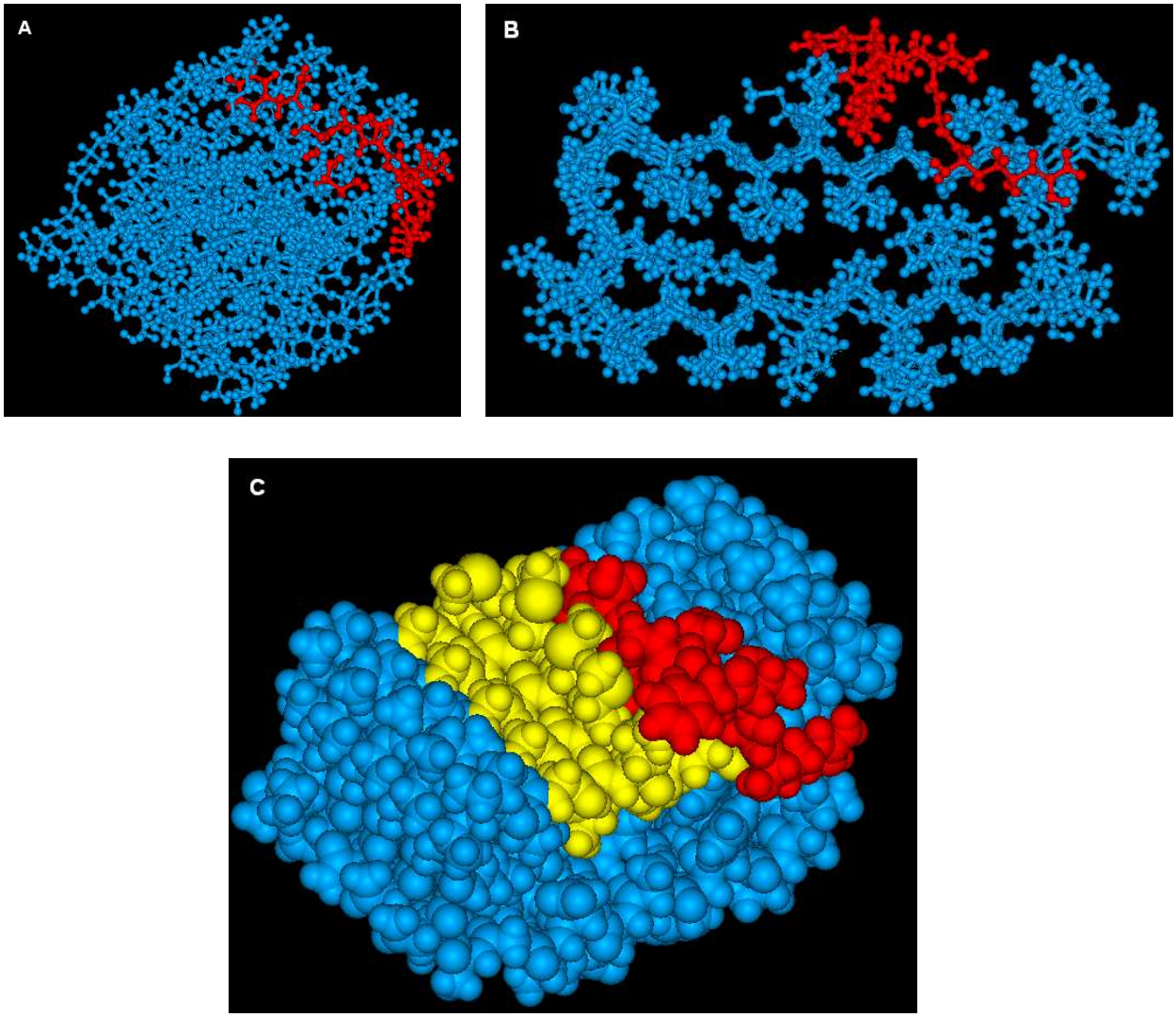

FIGURE 3.1. 2 : (A-B) The complex of reference peptide (red molecule) and amyloid (blue molecule) from different sides. (C) The CPK Model of the complex. Peptide is in red and amyloid is in blue. The yellow region shows the GxMxG motif in the surface

3.2. SIMULATION RESULTS

3.2.1. FIXATION – NPT SIMULATION

For the fixation step in the minimization process at constant temperature and constant pressure, the volume change was checked. For the reference peptide, RGTFEGKF, the volume decreased from 392500 $\mathring{A}^3$ to approximately 355000$\mathring{A}^3$. For the modified version RVTWEGKF (second peptide in Table 1) of it, the volume decreased from 357500 $\mathring{A}^3$ to 32000$\mathring{A}^3$.

3.2.2 THE CANONICAL ENSEMBLE

During NVT simulations, the complex of protein and peptide was aligned according to protein and RMSD change of peptide was considered. The designed peptide (AB1) found its stable conformation and binding region faster than the reference peptide (INH1).Therefore, a longer NVT simulation was performed for INH1.

For SMD, sample conformations of designed peptide (RVTWEGKF) were taken from interval 2.5 - 5 ns. Since the reference peptide did not find its stable conformation, sample conformations were taken from interval between 7.50 – 9.75 ns. There was 0.25 time difference between conformations.

3.3. STEERED MOLECULAR DYNAMICS

As a result of steered molecular dynamic simulations, work that is done on peptides was calculated with $W = F \times v \times \Delta t$. Here, F is force in$pN$; v is in $\AA/ps$ and Δt is time inps. Thus, work can be calculated in terms of joule. In order to convert joule to kcal/mol, it must be multiplied with conversion unit of kcal and Avogadro number $(2{,}3109\ x\ 10^{-4}) \times (6{,}02 \times 10^{23})$. The pseudocode that was used in calculation of work is given in the below:

TABLE 4 : The pseudocode that uses $W = F \times v \times \Delta t$ formula and implies the work in kcal/mol

```
t = is the time step number
f = external force that is applied to peptide
w(1) =  (10^-27)xf(1)x6.02x(10^23)x2.3901x(10^-4);
for i = 2 to (total number of time step)
     w(i) = w(i-1)+(10^-27)xf(i)x 6.02x(10^23)x2.3901x(10^-4);
end
```

When calculated work in terms of kcal/mol is plotted along trajectories: see Graph 3.3.1 and Graph 3.3.2 are obtained.

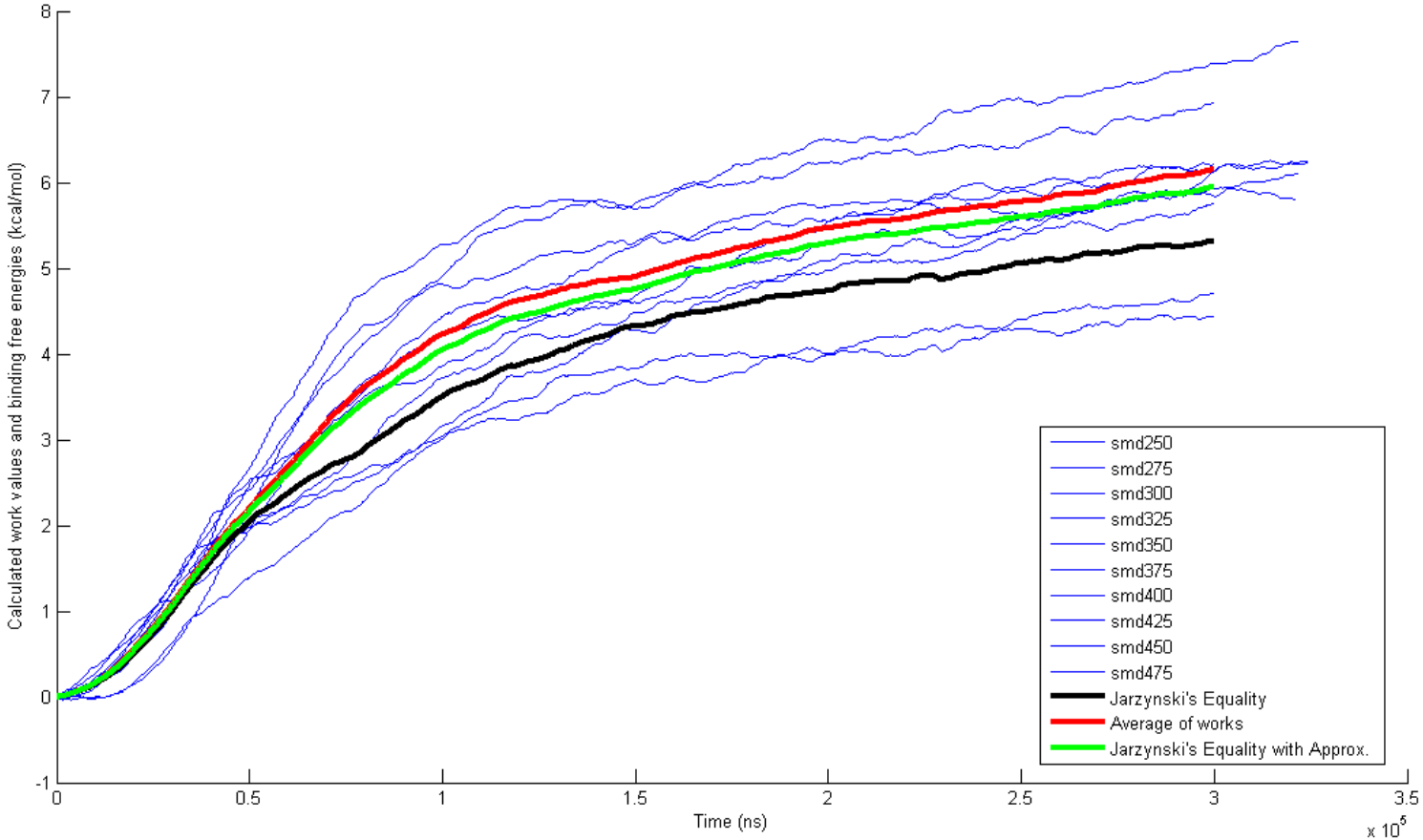

Graph 3.3. 1 : Work (kcal/mol) that is done by external forces on sample conformations of the designed peptide and binding free energy that is calculated with three different methods

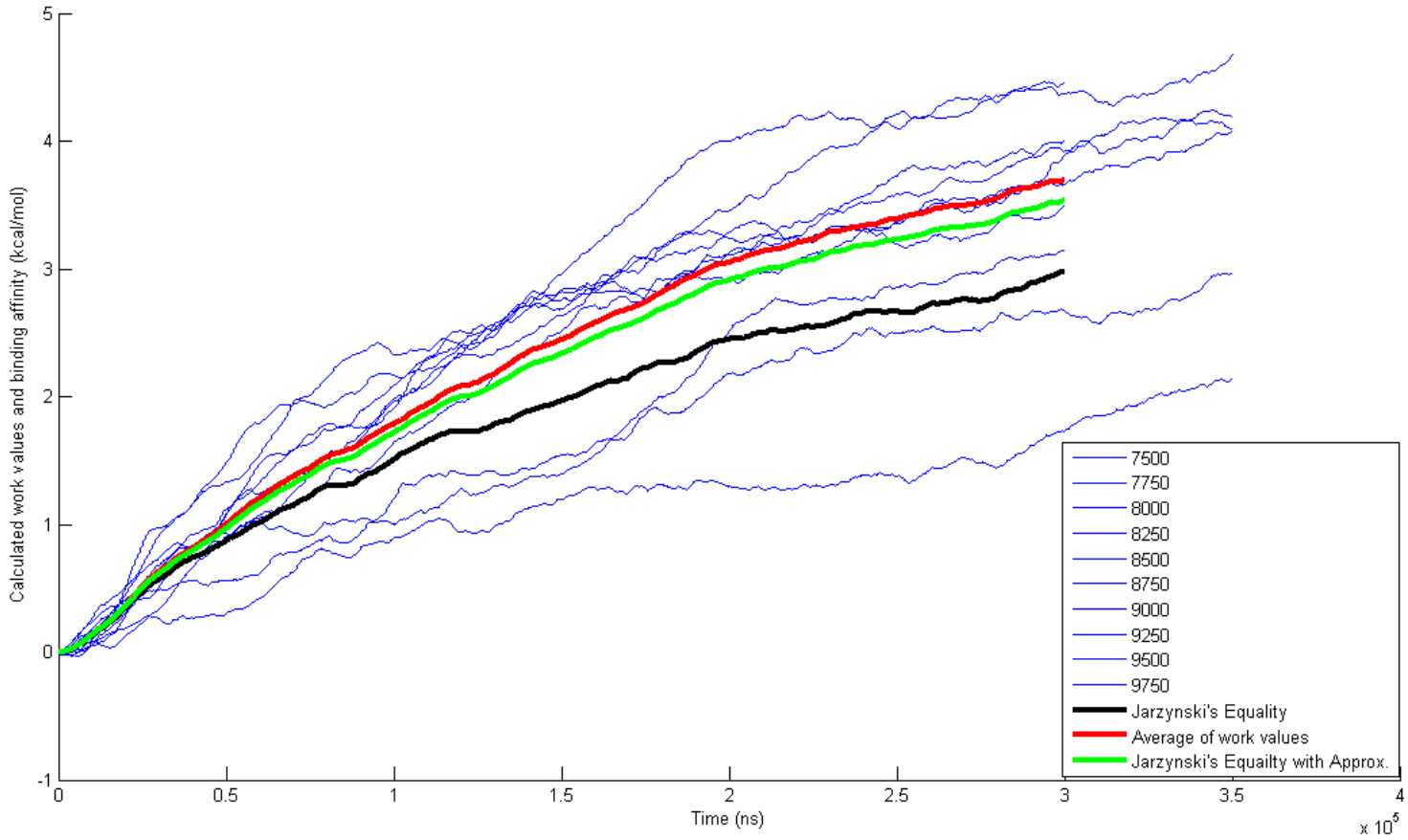

Graph 3.3. 2: Work (kcal/mol) that is done by external forces on sample conformations of the reference peptide and binding free energy that is calculated with three different methods

3.4. POTENTIAL OF MEAN FORCE

The comparison of binding free energies of two peptides which were calculated with Eq. 2.12 is shown in Graph 3.4.1

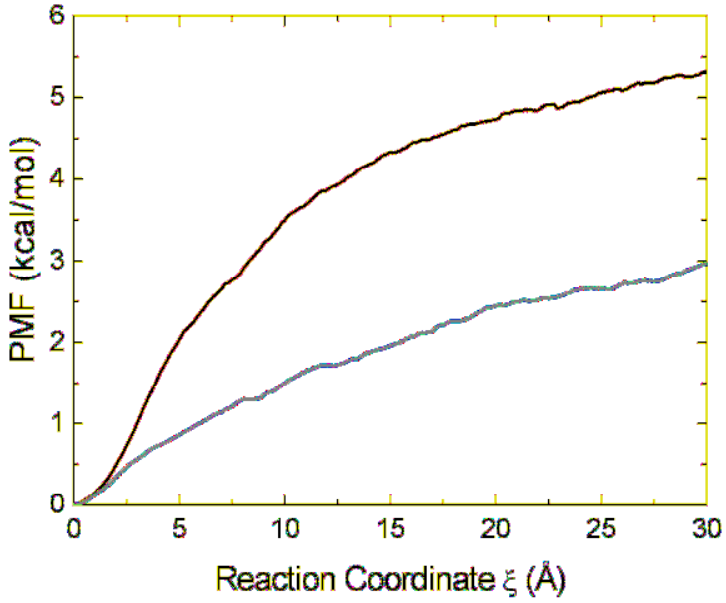

Graph 3.4 1 : Binding free energies of two peptide. (The values were obtained by using second order cumulant expansion in calculating Jarzynski's Equality)

CHAPTER 4

ANALYSIS OF RESULTS

When the docking results of variants of the reference peptide that were obtained by amino acid replacements are compared, it can be stated that replacements with a more hydrophobic amino acid according to Kyte and Doolittle [92] generally result in higher scores. For instance, the replacements of Glycine, with Valine and Isoleucine that are more hydrophilic than glycine provide higher docking scores. Another feature of valine or Isoleucine that contributes to the interactions and increases the score may be the longer side chain. The replacement of lysine in the seventh position with Arginine, that has extra $–NH_2$ groups and is more hydrophobic also gives a better binding.

However, there are also exceptions. For example, when Theroine in the third residue is replaced with serine that has a less hydropathy index, a higher score is obtained. Additionally, the replacement of phenylalanine in the fourth and last residues with tryptophan that is more hydrophilic increases the docking scores. But, when Phenylalanine is replaced with tyrosine that is more hydrophilic than phenylalanine and tryptophan, the docking score drops.

Another exception is the change of glutamate with glutamine. Glutamate has a negatively charged side chain, whereas glutamine has an uncharged polar side chain. Their hydropathy index is the same and -3.5, but the usage of glutamine increases the score.

The reason for obtaining higher scores with more hydrophobic amino acids may be the hydrophobicity of residues in amyloid surface. As given in Table 2, the residues of the reference peptide was mainly replaced more hydrophobic amino acids in the same amino acid group by considering hydrophobic characteristic of amyloid protofilament subunit. Additionally, interactions of amino acids also changed with replacements and this resulted in a different 3D structure. Therefore, the change of interaction within the peptide sequence with a different amino acid may also play a role in the increase of its score by causing a more compatible 3D structure for GxMxG motif on the amyloid protein.

The second peptide in Table 2 (AB1) was chosen according to its docking score and binding region. It fills the grooves that are composed by subsequent GxMxG motifs. Therefore, it prevents the binding of another amyloid. The reference peptide (INH1) can also fit in the groove partially and this positioning breaks possible interactions between two amyloid protofilament subunits. At the same time, they have similar physical and chemical properties. In order to analyze the binding process and obtain more accurate results, the two peptide-protein complex is investigated with molecular dynamics simulations.

As a result of the first two steps, the designed peptide (AB1) has reached its stable conformation faster than the reference peptide. In addition to this, the reference peptide (INH1) did not find its main binding region for a long time and its position changed a lot. Therefore, a longer NVT simulation for the reference peptide (INH1) was performed considering RMSD convergence of the peptide sequence. This shows that docking result of the designed peptide is more close to realistic case, and it could find its stable conformation and permanent binding region in a short time.

According to the results of steered molecular dynamics simulations, it can be clearly claimed that the designed peptide (AB1) binds amyloid stronger than reference peptide. Unbinding of the designed peptide requires a bigger force. By using the Jarzynski's Equality, binding free energy of the reference peptide was calculated as -2.98 kcal/mol; on the other hand binding free energy of designed peptide was calculated as -5.3 kcal/mol. Therefore, it can be stated that steered molecular dynamics simulations has confirmed comparison of docking results of two peptides. In addition to interaction with GxMxG motifs on amyloid surface, another reason that it effects on the difference between two calculated binding free energies may be the difference between NVT simulations. Since the reference peptide tried different conformations during the long NVT simulation, sample snapshots which were used in steered molecular dynamics simulations were less similar than the snapshots of the designed peptide.

However, magnitude of binding affinity, which is calculated with steered molecular dynamics is inconsistent with docking programs. GOLD calculated the binding affinity as approximately -15 kJ/mol and AutoDock calculated it as -8.7 kcal/mol. The possible reason for this may be the equilibration process in molecular dynamics simulations. In this process,

peptides did not stay in the exactly same conformation that they had taken in the docking programs, where they also changed their position. Thus, peptides in a different conformation and position were pulled in simulations.

As a result of the entire study, the designed peptide which is a derivative of the reference peptide binds to amyloid plaques successfully and with a higher affinity. Moreover, the calculated binding affinity is much greater than that of the reference peptide that is experimentally proved as effective. The designed peptide is expected to increase the ratio of survival of cells with Alzheimer's disease, since it has similar physical and chemical properties with the reference peptide.

CHAPTER 5

CONCLUSION

In the cross-β fibril structure of amyloid proteins, individual β strands have in-register and parallel arrangement and consecutive repeats of GxxxG motif form molecular ridges and grooves in the surface. This motif is also present in prion protein and α-synuclein protein. It has been shown that the amino acids with large side chains form molecular ridges, which fit in glycine grooves, and therefore this match between surfaces stabilizes fibril formation.

In order to break this compatibility between two amyloid surfaces, an 8-residue peptide RGTFEGKF was successfully designed and its inhibition effect was studied experimentally. Thus, this peptide and its derivatives were proven to be effective inhibitors against amyloid aggregation.

The aim of the present study that had motivated by the success of the experiments was to develop effective inhibitors and to investigate newly designed peptides' binding to amyloid with computational methods. In order to obtain derivatives of reference peptide, its amino acids were replaced with other amino acids that have the same characteristics. Thus, a small peptide library was obtained, and the peptide sequences in this library were docked to amyloid protofilament subunit. According to docking scores and physical and chemical similarity, the best result was chosen.

The two amyloid-peptide complexes were minimized and equilibrated. Then, peptides were pulled with an external force. The free energy change during this unbinding process was calculated with the Jarzynski's Equality that states Helmholtz free-energy difference between two equilibrium configurations of a system may be obtained from an ensemble of *finite-time* (nonequilibrium) measurements of the work performed in switching an external parameter of the system.

As a result of this study, it is shown that the newly designed peptide binds the amyloid protofilament subunit stronger than the reference peptide. Additionally, it completely fits the surface of glycine grooves on the amyloid surface whereas the reference peptide partially fits on the surface. Since these findings are the results of computational methods that simulate real systems with approximations, these must be confirmed experimentally. Furthermore, this study would probably provide more options to investigate other peptides that are successful in binding to the amyloid protofilament according to docking results. Investigating these steps may be the future work of this study.

APPENDIX A

The configuration file that was used for minimization:

```
#############################################################
## INPUT AND OUTPUT FILES                   ##
#############################################################

structure         ../common/1t_ionized.psf
coordinates       ../common/1t_ionized.pdb
set temperature    310
set outputname     1t
set restartname    res

firsttimestep      0
paraTypeCharmm                on
parameters          ../common/par_all27_prot_lipid.inp
temperature         $temperature
##############################################################
## SIMULATION PARAMETERS                                    ##
##############################################################
# Periodic Boundary Conditions
cellBasisVector1     97.8     0.     0.
cellBasisVector2      0.     67.5     0.
cellBasisVector3      0.     0.     59.6
cellOrigin          25.192     -11.358     1.119
wrapWater           on
wrapAll             on

# Force-Field Parameters
exclude             scaled1-4
1-4scaling          1.0
cutoff             12.
switching           on
switchdist          10.
pairlistdist       13.5

# Integrator Parameters
timestep            1.0
rigidBonds          off
nonbondedFreq       1
fullElectFrequency  1
stepspercycle       5

# PME (for full-system periodic electrostatics)
PME                 yes
PMEGridSizeX        100
PMEGridSizeY        72
PMEGridSizeZ        64

# Constant Temperature Control
langevin            on
langevinDamping     5
langevinTemp        $temperature
langevinHydrogen    on

# Constant Presssure control
```

```
useGroupPressure      yes
# is required in conjunction with rigidBonds
useFlexibleCell       no
useConstantArea       no

LangevinPiston        on
LangevinPistonTarget  1.01325
LangevinPistonPeriod  100.
LangevinPistonDecay   50.
LangevinPistonTemp    $temperature
#############################################################
## EXTRA PARAMETERS                                        ##
#############################################################
# Output
outputName          $outputname
restartName         $restartname
outputEnergies      100
outputPressure      100
restartfreq         100
dcdfreq             100
xstFreq             100

minimize 50000
reinitvels          $temperature
```

APPENDIX B

The configuration file that was used in fixation step in minimization process :

```
#######################################################
## INPUT AND OUTPUT FILES                            ##
#######################################################
structure         ../common/1t_ionized.psf
coordinates       ../common/1t_ionized.pdb
set temperature    310
set outputname     1t
set restartname    res
set ref_fix       ../common/reffix.pdb


firsttimestep      0
# Input
paraTypeCharmm                on
parameters          ../common/par_all27_prot_lipid.inp
temperature         $temperature
#############################################################
## SIMULATION PARAMETERS                                   ##
#############################################################
# Periodic Boundary Conditions
cellBasisVector1     97.8     0.     0.
cellBasisVector2      0.     67.5     0.
cellBasisVector3      0.     0.     59.6
cellOrigin          25.192     -11.358     1.119
wrapWater           on
wrapAll             on
```

```
# Force-Field Parameters
exclude             scaled1-4
1-4scaling          1.0
cutoff              12.
switching           on
switchdist          10.
pairlistdist        13.5


# Integrator Parameters
timestep            1.0
rigidBonds          off
nonbondedFreq       1
fullElectFrequency  1
stepspercycle       5


# PME (for full-system periodic electrostatics)
PME                 yes
PMEGridSizeX        100
PMEGridSizeY        72
PMEGridSizeZ        64


# Constant Temperature Control
langevin            on
langevinDamping     5
langevinTemp        $temperature
langevinHydrogen    on

# Constant Presssure control

useGroupPressure      yes
# is required in conjunction with rigidBonds
useFlexibleCell       no
useConstantArea       no

LangevinPiston        on
LangevinPistonTarget  1.01325
LangevinPistonPeriod  100.
LangevinPistonDecay   50.
LangevinPistonTemp    $temperature
#####################################################################
## EXTRA PARAMETERS                                 ##
#####################################################################
fixedAtoms on
fixedAtomsFile $ref_fix
fixedAtomsCol B


# Output
outputName          $outputname
restartName         $restartname
outputEnergies      100
outputPressure      100
restartfreq         100
dcdfreq             100
xstFreq             100
```

```
minimize 30000
reinitvels          $temperature
```

APPENDIX C

The configuration file that was used in NPT simulation :

```
#############################################################
## INPUT AND OUTPUT FILES                    ##
#############################################################

structure          ../common/ab1_ionized.psf
coordinates        ../common/ab1_ionized.pdb
set temperature    310
set outputname     ab1
set restartname    res
bincoordinates   ../..../res.coor
binvelocities    ../…/res.vel
extendedSystem   ../…/res.xsc

firsttimestep      0
# Input
paraTypeCharmm                on
parameters          ../common/par_all27_prot_lipid.inp
#temperature         $temperature
#############################################################
## SIMULATION PARAMETERS                    ##
#############################################################
# Periodic Boundary Conditions
cellBasisVector1     76.1     0.     0.
cellBasisVector2      0.     66.1     0.
cellBasisVector3      0.     0.     61.1
cellOrigin          -6.1     11.4     -5.7
wrapWater           on
wrapAll             on


# Force-Field Parameters
exclude             scaled1-4
1-4scaling          1.0
cutoff              12.
switching           on
switchdist          10.
pairlistdist        13.5


# Integrator Parameters
timestep            1.0
rigidBonds          off
nonbondedFreq       1
fullElectFrequency  1
stepspercycle       5


# PME (for full-system periodic electrostatics)
```

```
PME             yes
PMEGridSizeX    80
PMEGridSizeY    72
PMEGridSizeZ    64


# Constant Temperature Control
langevin        on
langevinDamping  5
langevinTemp     $temperature
langevinHydrogen  on


# Constant Presssure control
useGroupPressure     yes
# is required in conjunction with rigidBonds
useFlexibleCell      no
useConstantArea      no

LangevinPiston       on
LangevinPistonTarget  1.01325
LangevinPistonPeriod  100.
LangevinPistonDecay   50.
LangevinPistonTemp    $temperature
#############################################################
## EXTRA PARAMETERS                                        ##
#############################################################
# Output
outputName         $outputname
restartName        $restartname
outputEnergies     2000
outputPressure     2000
restartfreq        2000
dcdfreq            2000
xstFreq            2000

run 500000
```

APPENDIX D

The configuration file that was used in NVT simulation :

```
#######################################################
## INPUT AND OUTPUT FILES                            ##
#######################################################
structure        ../common/ab1_ionized.psf
coordinates      ../common/ab1_ionized.pdb
set temperature   310
set outputname    ab1
set restartname   res
bincoordinates   ../…/res.coor
binvelocities    ../…/res.vel
extendedSystem   ../…/res.xsc

firsttimestep     0
# Input
```

```
paraTypeCharmm              on
parameters          ../common/par_all27_prot_lipid.inp
#temperature         $temperature
#############################################################
## SIMULATION PARAMETERS                                   ##
#############################################################
# Force-Field Parameters
exclude             scaled1-4
1-4scaling          1.0
cutoff              12.
switching           on
switchdist          10.
pairlistdist        13.5


# Integrator Parameters
timestep            1.0
rigidBonds          off
nonbondedFreq       1
fullElectFrequency  1
stepspercycle       5

# PME (for full-system periodic electrostatics)
PME                 yes
PMEGridSizeX        80
PMEGridSizeY        72
PMEGridSizeZ        64
wrapAll on

# Constant Temperature Control
langevin            on
langevinDamping     5
langevinTemp        $temperature
langevinHydrogen    on

#############################################################
## EXTRA PARAMETERS                                        ##
#############################################################
# Output
outputName          $outputname
restartName         $restartname
outputEnergies      100
outputPressure      100
restartfreq         100
dcdfreq             100
xstFreq             100

run 500000
```

APPENDIX E

The configuration file that was used in SMD simulations :

```
#######################################################
## INPUT AND OUTPUT FILES                            ##
#######################################################
structure          ../common/1t_ionized.psf
```

```
coordinates       ../common/1t182.pdb
set temperature    310
set outputname     1t182
set restartname    res
set ref_smd      ../common/smdref_182.pdb
extendedSystem   ../common/res.xsc

firsttimestep      0
# Input
paraTypeCharmm                on
parameters          ../common/par_all27_prot_lipid.inp
temperature         $temperature
##############################################################
## SIMULATION PARAMETERS                                    ##
##############################################################
if {1} {
cellBasisVector1    95.48    0.   0.
cellBasisVector2     0.   66.42   0.
cellBasisVector3     0.    0   58.83
cellOrigin          25.136    -11.280   1.160
}
wrapWater           on
wrapAll             on

# Force-Field Parameters
exclude             scaled1-4
1-4scaling          1.0
cutoff              12.
switching           on
switchdist          10.
pairlistdist        13.5

# Integrator Parameters
timestep            1.0
rigidBonds          off
nonbondedFreq       1
fullElectFrequency  1
stepspercycle       5

# PME (for full-system periodic electrostatics)
PME                 yes
PMEGridSizeX        100
PMEGridSizeY        72
PMEGridSizeZ        64

# Constant Temperature Control
langevin            on
langevinDamping     5
langevinTemp        $temperature
langevinHydrogen    on
##############################################################
## EXTRA PARAMETERS                                         ##
##############################################################
if {1} {
fixedAtoms          on
fixedAtomsFile      $ref_smd
fixedAtomsCol       B
}
SMD on
SMDFile $ref_smd
```

```
#Spring constant
SMDk 7
SMDVel 0.00001
SMDDir 0.932 -0.361 0.038
SMDOutputFreq 10

# Output
outputName          $outputname
restartName         $restartname
outputEnergies      2000
outputPressure      2000
restartfreq         2000
dcdfreq             2000
xstFreq             2000

run 3000000
```

BIBLIOGRAPHY

[1]. Berchtold NC, Cotman CW (1998). Evolution in the conceptualization of dementia and Alzheimer's disease: Greco-Roman period to the 1960s. *Neurobiol. Aging* **19** (3): 173–89.

[2]. Kalaria et al. (2008). Alzheimer's disease and vascular dementia in developing countries: prevalence, management, and risk factors. *Lancet Neurol*. **7**(9) : 812 – 826

[3]. Perez et al. (1975). Analysis of intellectual and cognitive performance in patients with multi-infarct dementia, vertebrobasilar insufficiency with dementia, and Alzheimer's disease. *Journal of Neurology, Neurosurgery, and Psychiatry*. **38**: 533-540

[4]. Web Site of Alzheimer's Research Trust (n.d). Alzheimer's diagnosis of AD. Retrieved from http://www.alzheimers-research.org.uk/info/diagnosis/ on 2010-05-05.

[5]. Wenk GL (2003). Neuropathologic changes in Alzheimer's disease. *J Clin Psychiatry* **64**(9): 7–10

[6]. Tiraboschi, P., Hansen, L.A., Thal, L.J., Corey-Bloom, J. (2004). The importance of neuritic plaques and tangles to the development and evolution of AD. *Neurology* **62** (11): 1984–9

[7]. Sato et al. (2006). Inhibitors of amyloid toxicity based on beta-sheet packing of Abeta40 and Abeta42. *Biochemistry*. **45**:5503–5516

[8]. Jones, G., Willett, P. & Glen, R. C. (1995). Molecular recognition of receptor sites using a genetic algorithm with a description of desolvation. *J. Mol. Biol.*, **245**: 43-53

[9]. Rodgers, A. B. (2003). Alzheimer's Disease : Unraveling the Mystery. National Institutes of Health Publications. Publication Number : 02-3782

[10]. Alzheimer's Association (2010). Alzheimer's Disease.

[11]. Ray et al. (2007). "Classification and prediction of clinical Alzheimer's diagnosis based on plasma signaling proteins". Nature Medicine, 13(11) : 1359- 1463

[12]. McKhann, G. (1984). "Clinical diagnosis of Alzheimer's disease". Neurology,34: 939-943

[13]. Petrella et al. (2003), "Neuroimaging and Early Diagnosis of Alzheimer Disease: A Look to the Future," *Radiology* 226(2) : 315-36.

[14]. Klunk et al. (2004). "Imaging brain amyloid in Alzheimer's disease with Pittsburgh Compound-B". *Ann Neurol*. **55** : 306 – 319

[15]. Mudher, A., Lovestone, S. (2002). "Alzheimer's disease-do tauists and baptists finally shake hands?". *Trends Neurosci.* **25** (1): 22–26

[16]. Hardy J, Allsop D (1991). "Amyloid deposition as the central event in the aetiology of Alzheimer's disease". *Trends Pharmacol. Sci.* **12** (10): 383–88

[17]. Masliah et al.(1996). "Comparison of neurodegenerative pathology in transgenic mice overexpressing V717F beta-amyloid precursor protein and Alzheimer's disease". *J Neurosci* **16** (18): 5795–81

[18]. Lalonde et al. (2002) "Spatial learning, exploration, anxiety, and motor coordination in female APP23 transgenic mice with the Swedish mutation.". *Brain Research* **956** (1): 36–44

[19]. Ferri, C. & Prince, M. (2005). “Statistics”, The Lancet, **366** : 2112 – 2117

[20]. Stahl SM (2000). "The new cholinesterase inhibitors for Alzheimer's disease, Part 2: illustrating their mechanisms of action". *J Clin Psychiatry* **61** (11): 813–814

[21]. Web Site of National Library of Medicine (Medline Plus)(2010). “Donepezil”. Retrieved from http://www.nlm.nih.gov/medlineplus/druginfo/meds/a697032.html on 2010-05-05

[22]. Web Site of National Library of Medicine (Medline Plus)(2010). “Galantamine”. Retrieved from http://www.nlm.nih.gov/medlineplus/druginfo/meds/a699058.html on 2010-05-05

[23]. Web Site of National Library of Medicine (Medline Plus)(2010). “Riyastigmine”. Retrieved from http://www.nlm.nih.gov/medlineplus/druginfo/meds/a602009.html on 2010-05-05

[24]. Eisai and Pfizer. (2007). "Aricept Prescribing information" . Retrieved from http://www.aricept.com/images/AriceptComboFullPINovember02006.pdf on 2010-05-05

[25]. Ortho-McNeil Neurologics. (2007). "Razadyne ER U.S. Full Prescribing Information". Retrieved from http://razadyneer.com/razadyneer/pages/pdf/razadyne_er.pdf on 2010-05-05

[26]. Novartis Pharmaceuticals. (2007). "Exelon ER U.S. Prescribing Information" . Retrieved from www.pharma.us.novartis.com/product/pi/pdf/exelonpatch.pdf on 2010-05-05

[27]. Food and Drug Administration. (2007). “Exelon Warning Letter”. Retrieved from http://www.fda.gov/downloads/Drugs/GuidanceComplianceRegulatoryInformation/EnforcementActivitiesbyFDA/WarningLettersandNoticeofViolationLetterstoPharmaceuticalCompanies/ucm054180.pdf on 2010-05-05

[28]. Siegel et al. (1999). Basic Neurochemistry (6^{th} Edition). Philadelphia: Lippincott-Raven

[29]. Hartmann et al.(1997). "Distinct sites of intracellular production for Alzheimer's disease A beta40/42 amyloid peptides". *Nat. Med.* **3** (9): 1016–20.

[30]. Luhrs et al.(2005). “3D structure of Alzheimer’s amyloid-beta (1–42) fibrils”. *Proc. Natl. Acad. Sci.* **102**:17342–17347.

[31]. Ma, B., and R. Nussinov.(2002). “Stabilities and conformations of Alzheimer’s beta-amyloid peptide oligomers (Abeta 16–22, Abeta 16–35, and Abeta 10–35): sequence effects”. *Proc. Natl. Acad. Sci.* **99**:14126–14131

[32]. Petkova, A. T., W. M. Yau, and R. Tycko. 2006. Experimental constraints on quaternary structure in Alzheimer's beta-amyloid fibrils. *Biochemistry*. **45**:498–512.

[33]. Butterfield, D. A., and A. I. Bush. 2004. Alzheimer's amyloid betapeptide(1–42): involvement of methionine residue 35 in the oxidative stress and neurotoxicity properties of this peptide. *Neurobiol. Aging*. **25**:563–568.

[34]. Barnham et al (2004). Enhanced toxicity and cellular binding of a modified amyloid fbetag peptide with a methionine to valine substitution. *J. Biol. Chem*. **279**:42528–42534.

[35]. Vivien, M. (2005). "Watching Peptide Drugs Grow Up". Chemical &Engineering news, **83**(11) : 17- 24

[36]. Kurumbail et al. (2002). "Molecular docking and high-throughput screening for novel inhibitors of protein tyrosine phosphatase-1B". *J Med Chem* **45**: 2213–2221

[37]. Hoffman et al. (2007). "A fragment-based approach for the discovery of isoform-specific p38alpha inhibitors". ACS *Chem Biol* **2**: 329–336.

[38]. Carr, R.A., Congreve, M., Murray, C.W., Rees DC (2005). "Fragment-based lead discovery: leads by design". *Drug Discov Today*, **10**: 987–992.

[39]. Hann MM, Leach AR, Harper, G. (2001). "Molecular complexity and its impact on the probability of finding leads for drug discovery". *J Chem Inf Comput Sci* **41**: 856–864.

[40]. Jones, G., Willett, P., Glen, R.C. (1995) "Molecular recognition of receptor sites using a genetic algorithm with a description of desolvation". *J Mol Biol* **245**: 43–53.

[41]. Taylor et al (1997) Development and validation of a genetic algorithm for flexible docking. *J Mol Biol* **267**: 727–748.

[42]. Ewing TJ, Makino S, Skillman AG, Kuntz ID (2001) DOCK 4.0: search strategies for automated molecular docking of flexible molecule databases. *J Comput Aided Mol Des* **15**: 411–428.

[43]. Goodsell DS, Morris GM, Olson AJ (1996) Automated docking of flexible ligands: applications of AutoDock. *J Mol Recognit* **9**: 1–5.

[44]. Halgren TA, Murphy RB, Friesner RA, Beard HS, Frye LL, et al. (2004) Glide: a new approach for rapid, accurate docking and scoring. 2. Enrichment factors in database screening. *J Med Chem* **47**: 1750–1759.

[45]. Klicic et al. (2004) Glide: a new approach for rapid, accurate docking and scoring. 1. Method and assessment of docking accuracy. *J Med Chem* **47**: 1739–1749.

[46]. Rarey M, Kramer B, Lengauer T, Klebe G (1996). "A fast flexible docking method using an incremental construction algorithm". *J Mol Biol* **261**: 470–489.

[47]. Bursulaya, B.D., Totrov M, Abagyan R, Brooks, C.L. (2003). “Comparative study of several algorithms for flexible ligand docking”. *J Comput Aided Mol Des,* **17**: 755–763.

[48]. Stahl M, Rarey M (2001). “Detailed analysis of scoring functions for virtual screening”. *J Med Chem,* **44**: 1035–1042.

[49]. Locher et al. (2003). “Novel dihydrofolate reductase inhibitors. Structure-based versus diversity-based library design and high-throughput synthesis and screening”. *J Med Chem*, **46**: 2304–2312.

[50]. Pearlman, D.A., Charifson, P.S. (2001). “Are free energy calculations useful in practice? A comparison with rapid scoring functions for the p38 MAP kinase protein system”. *J Med Chem* **44**: 3417–3423.

[51]. Morimoto et al. (2009) High-Performance Drug Discovery: Computational Screening by Combining Docking and Molecular Dynamics Simulations. *PLoS Comput Biol **5(***10): e1000528.

[52]. Karplus, M. & McCammon, J. A. (2002). “Molecular dynamics simulations of biomolecules”. *Nat. Struct. Biol.* **9**: 646–652.

[53]. Schlick, T. (1996). "Pursuing Laplace's Vision on Modern Computers". in J. P. Mesirov, K. Schulten and D. W. Sumners. *Mathematical Applications to Biomolecular Structure and Dynamics, IMA in Mathematics and Its Applications*. **82**. New York: Springer-Verlag. pp. 218–247.

[54]. Allen, M. P. (2004). “Introduction to Molecular Dynamic Simulations”. *NIC Series, Vol.* **23**: 1-28

[55]. Grossfield, A., Feller, S. E & Pitman, C. M. (2007). “Convergence of molecular dynamics simulations of membrane proteins” *Proteins: Struct. Funct. Bioinf.*, **67:** 31−40.

[56]. Zanuy et al. (2004). “Insights into amyloid structural formation and assembly through computational approaches”. *Amyloid, **11*** (3) : 143 – 161

[57]. Buchete, N. V., Tycko, R & Hummer, G. (2005). “Molecular Dynamics Simulations of Alzheimer’s b-Amyloid Protofilaments”. J. *Mol. Biol*.,**353**: 804–821

[58]. Lührs et al. (2005). “3D structure of Alzheimer’s amyloid-β(1– 42) fibrils.” *PNAS*, **102** (48) : 17342–17347

[59]. Tycko R. (2006). “Molecular structure of amyloid fibrils: Insights from solid-state NMR”. *Q Rev Biophys* , **39**:1–55.

[60]. Török, M. (2002). “Structural and Dynamic Features of Alzheimer's Aβ Peptide in Amyloid Fibrils Studied by Site-directed Spin Labeling”. *Journal of Biological Chemistry*, **277**, 40810-40815

[61]. Harmeier et al (2009). "Role of Amyloid-_ Glycine 33 in Oligomerization, Toxicity, and Neuronal Plasticity". *The Journal of Neuroscience*, **29**(23):7582–7590

[62]. Florio et al. (2003). "Contribution of two conserved glycine residues to fibrillogenesis of the 106-126 prion protein fragment. Evidence that a soluble variant of the 106-126 peptide is neurotoxic". *J Neurochem.* **85**(1):62-72

[63]. Biere et al. (2000). "Parkinson's Disease-associated α-Synuclein Is More Fibrillogenic than β- and γ-Synuclein and Cannot Cross-seed Its Homologs". *J Biol Chem*, **275**: 34574-34579

[64]. Jones, G., Willett, P., Glen, R.C. (1995) "Molecular recognition of receptor sites using a genetic algorithm with a description of desolvation". *J Mol Biol* **245**: 43–53.

[65]. Nissink et al. (2002). "A new test set for validating predictions of protein ligand interaction". *Proteins*, **49**, 457-471

[66] Mee et al. (1997). "Empirical scoring functions: I. The development of a fast empirical scoring function to estimate the binding affinity of ligands in receptor complexes".*J Comput Aided Mol Des* 1997 , **11**(5)**:**425-445

[67]. Lindahl, E. R. (2008). "Molecular modeling of proteins". *Methods in Molecular Biology*, **443** : 63-88.

[68]. Joung, I. S. & Cheatham, T. E.(2008)."Determination of Alkali and Halide Monovalent Ion Parameters for Use in Explicitly Solvated Biomolecular Simulations". *J.Phys.Chem B*,**112** : 9020

[69]. Nina, M., Beglov, D., Roux, B.(1994). "Atomic Radii for Continuum Electrostatics Calculations Based on Molecular Dynamics Free Energy Simulations". *J. Chem. Phys*, **100**: 9050.

[70]. Jorgensen, W. L., Maxwell, D. S., Tirado-Rives, J. (1996). "Development and Testing of the OPLS All-Atom Force Field on Conformational Energetics and Properties of Organic Liquids" *J. Am. Chem. Soc.* ***118***, 11225

[71]. Dang, L. X.(1995). "Mechanism and Thermodynamics of Ion Selectivity in Aqueous Solutions of 18-Crown-6 Ether: A Molecular Dynamics Study". *J. Am. Chem. Soc.*, ***117***, 6954

[72]. Berendsen, H. J. C., Grigera, J. R., Straatsma, T. P.(1987). "The missing term in effective pair potentials" *J. Phys. Chem.* 1987, *91*, 6269

[73]. Klein et al. (1983). "Comparison of simple potential functions for simulating liquid water". *J. Chem. Phys* , **79**, 926-935

[74]. Schulten et al (2005). Scalable molecular dynamics with NAMD. *Journal of Computational Chemistry*, **26**: 1781-1802.

[75]. MacKerell, Jr. A.D., Banavali, N., Foloppe, N. (2001). "Development and current status of the CHARMM force field for nucleic acids". *Biopolymers*, **56** (4): 257–265

[76]. NAMD Tutorial.(2009). Theoretical and Computational Biophysics group, an NIH Resource for Macromolecular Modeling and Bioinformatics, Beckman Institute, University of Illinois at Urbana-Champaign. [cited; http://www.ks.uiuc.edu/]. Available from: http://www.ks.uiuc.edu/.

[77]. Allen, M.P. and Tildesley, D. J.,(1987). "Periodic Boundary Conditions" and "Potential Truncation." In: *Computer Simulations of Liquids*, Oxford University Press, Oxford

[78]. Andersen, H. C. (1980). "Molecular dynamics simulations of the liquid-crystal phases of 2-(4-butyloxyphenyl)-5-octyloxypyrimidine and 5-(4-butyloxyphenyl)-2 - octyloxypyrimidine". J. Chem. Phys. **72**, 2384

[79]. Feller, S. C., Zhang, Y., Pastor R. W., Brooks, B. R. (1995). "Constant pressure molecular dynamics simulation: The Langevin piston method". J. Chem. Phys. **103**, 4613

[80]. Strynadka et al (1995). "A potent new mode of β-lactamase inhibition revealed by the 1.7 Å resolution structure of the TEM-1/BLIP complex." *Nature Struct. Biol.* **3**, 290−297

[81]. McCammon and Harvey, 1987

[82]. Ajay, M. & Mark, M.(1995). "Computational Methods to Predict Binding Free Energy in Ligand-Receptor Complexes". *J. Med. Chem.*, ***38*** (26) : 4953 - 4967

[83] Gilson et al.(1994). "Open back door in a molecular-dynamics simulation of acetylcholinesterase.". *Science.* **263**:1276–1278.

[84]. Schulten et al. (1998) "Steered molecular dynamics," in *Computational Molecular Dynamics: Challenges, Methods, Ideas*, edited by P. Deuflhard, J. Hermans, B. Leimkuhler, A. E. Mark, S. Reich, and R. D. Skeel, Lecture Notes in Computational Science and Engineering (Springer-Verlag, Berlin), **4**: 36–62.

[85]. Parket al., (2003). Free energy calculation from steered molecular dynamics simulations using Jarzynski's equality. *Journal of Chemical Physics*, **119**(6): 3559-3566.

[86]. Jarzynski, C.,(1997) Equilibrium free-energy differences from nonequilibrium measurements: A master-equation approach. *Physical Review E*, **56**(5): 5018-5035.

[87].Jarzynski, C.,(1997) Nonequilibrium equality for free energy differences. *Physical Review Letters*, **78**(14): 2690-2693

[88]. Jensen et al.,(2002). Energetics of glycerol conduction through aquaglyceroporin GlpF. PNAS, **99**(10): 6731-6736.

[89]. Hummer, G.,(2001) Fast-growth thermodynamic integration: Error and efficiency analysis. Journal of Chemical Physics, **114**(17): 7330-7337.

[90]. Park, S. and Schulten, K. (2004). Calculating potentials of mean force from steered molecular dynamics simulations. *Journal of Chemical Physics*, **120**(13): 5946-5961

[91] Trott,O & Olson, A. J. (2010). AutoDock Vina: Improving the speed and accuracy of docking with a new scoring function, efficient optimization, and multithreading. *Journal of Computational Chemistry*, 31(2): 455–461

[92] Kyte, J., Doolittle, R.F. (1982). "A simple method for displaying the hydropathic character of a protein." J Mol Biol., **157**(1):105-32.

VITA

Gözde Eskici was born in Samsun, Turkey in 1986. She received her Bachelor of Science Degree in Molecular Biology and Genetics from Istanbul Technical University. In September 2008, she attended Computational Sciences and Engineering M.S. program at Koç University. From 2008 to 2010, she worked as research and teaching assistant at the same institution.